

# Statistical Volume Elements for Metal Foams

M. Geißendörfer, A. Liebscher, C. Proppe, C. Redenbach, and D. Schwarzer

**Abstract** Open cell metal foams can be represented by a network of beams. Due to the heterogeneity of the geometry, the length scale of the representative volume element is often nearly of the same order as the length scale of structures made of metal foam. Therefore, classical homogenization techniques for the computation of effective properties can not be applied. Statistical volume elements lead to apparent material properties that depend on the boundary conditions. Here, we introduce a model for structures made of metal foam that consists of two domains, an interior region and a boundary region. For both regions, unique random fields are identified by simulations of the microstructure. The model is validated by comparison with Finite Element simulations and experiments.

**Keywords** Metal foam • Stochastic analysis • Multiscale method • Modal analysis

## 1 Introduction

For heterogeneous materials, the size of the representative volume element can be quite large (Dirrenberger et al. 2014). In this case, the assumption of scale separation is not valid anymore. For metal foams, the representative volume element is estimated to consist of about 1,000 cells (Kanaun and Tkachenko 2007).

---

M. Geißendörfer (✉) • C. Proppe • D. Schwarzer  
Institute of Engineering Mechanics, Karlsruhe Institute of Technology, Karlsruhe, Germany  
e-mail: [maximilian.geissendoerfer@kit.edu](mailto:maximilian.geissendoerfer@kit.edu); [proppe@kit.edu](mailto:proppe@kit.edu); [schwarzer@kit.edu](mailto:schwarzer@kit.edu)

A. Liebscher • C. Redenbach  
Mathematics Department, University of Kaiserslautern, Kaiserslautern, Germany  
e-mail: [liebscher@mathematik.uni-kl.de](mailto:liebscher@mathematik.uni-kl.de); [redenbach@mathematik.uni-kl.de](mailto:redenbach@mathematik.uni-kl.de)

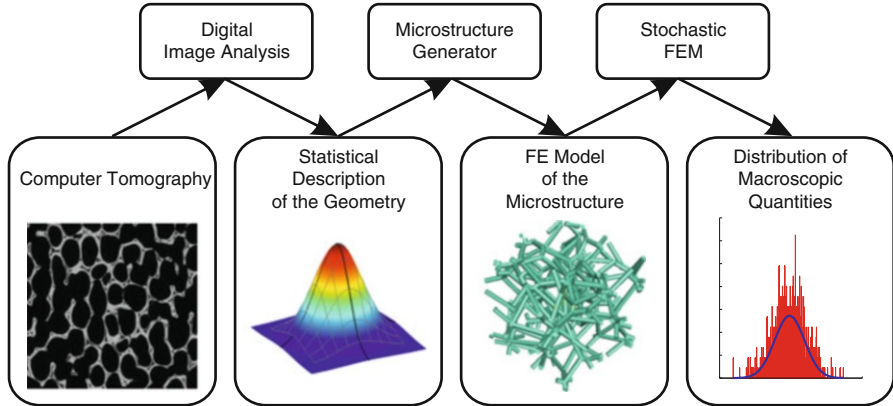


**Fig. 1** Overview of the proposed computational procedure

If scale separation can not be assumed, it is still possible to compute apparent material properties (Huet 1990) and to provide a macroscopic description by random fields (Guillemot et al. 2011). However, the apparent material properties depend on the boundary conditions. Therefore, a unique random field for the apparent material properties does not exist (Ostoja-Starzewski 2011). Recently, Di Paola (2011) proposed an averaging method that leads to unique boundary effect independent apparent properties. In this method, material properties are obtained by averaging over a volume that is smaller than the volume element on which the boundary conditions are applied.

Since the basic deformation mechanism is bending dominated, the mechanical model of metal foam is a three dimensional network of connected Timoshenko type beams with the material properties of the solid structure (Gibson and Ashby 1997). Averaging over a volume inside a beam network would predict a stiffer behavior than averaging over the whole volume element, due to the free, unconnected ends of the beams at the boundary of the volume element. Therefore, averaging over volumes smaller than the volume element will be valid only in the interior of a structure. For these reasons, a model for structures made of metal foam that consists of two domains – an interior region and a boundary region – is introduced and investigated here. In the interior region, a unique random field is identified that represents boundary effect independent apparent properties. For the boundary region, a random field is obtained by applying appropriate boundary conditions. The proposed approach allows to work with a uniquely defined random field by introducing a slightly more complex structural model.

For structures made of metal foam, uncertainties are mainly due to the heterogeneous geometry. By introducing suitable statistical volume elements, applying boundary conditions and an averaging procedure, uncertainties are propagated from the geometry to the material properties and to macroscopic structural behavior. This propagation process is sketched in Fig. 1. It applies also to other types of heterogeneous materials and macroscopic properties than those studied in this

paper. This paper is organized along the propagation process as follows: the next section discusses the microstructure model, Sects. 3 and 4 treat the generation and analysis of mesoscale volume elements. In Sect. 5, predictions are compared with experiments for an open cell copper foam and in Sect. 6, conclusions are drawn.

## 2 Microstructure

### 2.1 CT Analysis

As an example of application we investigate a Duocel<sup>®</sup> copper foam. A stochastic microstructure model is developed and adapted to the geometric characteristics estimated from three-dimensional  $\mu$ CT images. For that purpose, ten cubes of 25 mm side length were imaged by CT with a voxel edge length of 38.15  $\mu$ m. A visualization of one of the samples is shown in Fig. 2. The volume fraction of copper was on average 12.6%. Foam cells have been reconstructed by the following procedure (Ohser and Schladitz 2009): First, the images were binarized using a global threshold. On the resulting binary images, the Euclidean distance transform was applied which assigns to each cell pixel its distance to the nearest strut. Ideally, the resulting image has local maxima at the cell centers. In practice, however, additional maxima may appear due to discretization effects and irregular cell shapes. These were removed using an adaptable h-maxima transform. Finally, the watershed algorithm was applied to the inverted distance images to separate the single cells. All image processing steps were performed using the MAVI software package (Fraunhofer ITWM, Department Image Processing (Hrsg.) 2006).

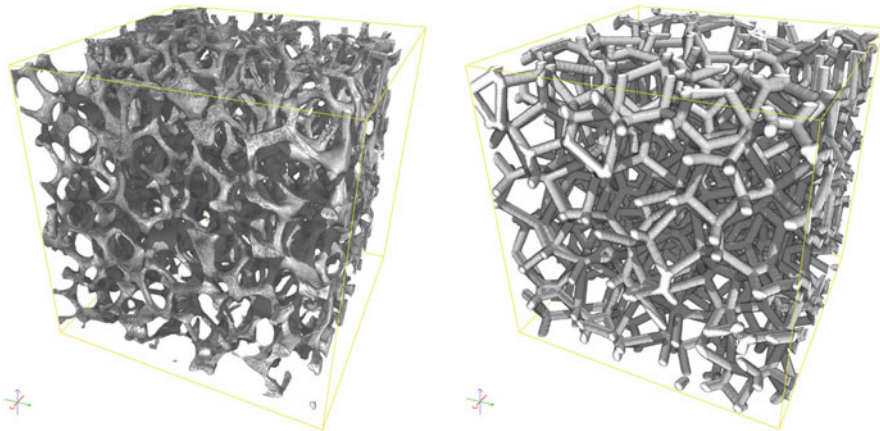


**Fig. 2** Visualizations of a CT image of the Cu Duocel<sup>®</sup> foam (*left*) and the model (*right*). Visualized are  $500^3$  voxels

**Table 1** Cell properties obtained from CT analysis

Property	Mean	Standard deviation
Diameter	5.09 mm	0.30 mm
Surface area	80.19 mm <sup>2</sup>	9.58 mm <sup>2</sup>
Volume	49.64 mm <sup>3</sup>	9.12 mm <sup>3</sup>
Facets	13.90	1.48

From the reconstructed cell systems, the geometric quantities summarized in Table 1 were estimated using minus-sampling edge correction (Ohser and Schladitz 2009). The mean number of cells per 1,000 mm<sup>3</sup> was 20.15. The mean cell diameters in the coordinate directions indicated an anisotropy in the cell structure. Although this can be included in the microstructure model (Redenbach 2009), a simplified model assuming isotropy of the microstructure was used here.

## 2.2 Microstructure Generation

Solid foams show a high variability in cell sizes and shapes, which influences their elastic properties (Zhu et al. 2000). This variability cannot be represented by deterministic models. Random tessellations (Stoyan et al. 1995) proved to be a suitable model class in this regard.

An important class of random tessellation models are Voronoi tessellations generated from realizations of random point processes. Voronoi tessellations generated by hard-core point processes are of particular interest for the modelling of foam cells due to their relatively regular cell shapes. However, the adaptability of the size distribution of the tessellation cells to the estimated size distribution is limited. To overcome this problem, weighted Voronoi tessellations can be considered. For modelling foam cells, Laguerre or power-tessellations (Aurenhammer 1987) are a promising model class. This model is defined as follows: given a set  $S$  of spheres, the Laguerre cell  $C(s(x, r), S)$  of a sphere  $s(x, r)$  in  $S$  with center  $x$  and radius  $r$  is defined as

$$C(s(x, r), S) = \{y \in \mathbb{R}^3 : \|y - x\|^2 - r^2 \leq \|y - x'\|^2 - r'^2, \forall s(x', r') \in S\}, \quad (1)$$

where  $\|\cdot\|$  denotes the Euclidean norm. The Laguerre tessellation is the set of all non-empty Laguerre cells of spheres in  $S$ . It forms a space-filling system of convex polytopes. If all spheres have equal radii, the Voronoi tessellation is obtained.

If the set  $S$  forms a system of non-overlapping spheres, each sphere is completely contained in its Laguerre cells. Consequently, the volume distribution of the spheres can, to a certain degree, be used to control the volume distribution of the cells. A method for adapting Laguerre tessellations generated by hard sphere packings to real foams based on the statistical analysis of CT images is presented in Redenbach (2009). The superiority of Laguerre tessellations over Poisson and hard-core

Voronoi tessellations has been shown in Lautensack (2008) and Hardenacke and Hohe (2010). Laguerre tessellations were used to determine the elastic properties of a representative volume element of metal foam in Kanaun and Tkachenko (2008) and Hardenacke and Hohe (2009).

Based on the data shown in Table 1, a Laguerre tessellation was fit to the foam structure using the procedure introduced in Redenbach (2009). A system of non-overlapping spheres simulated by the force-biased algorithm was chosen to reproduce the regularity of the observed cell shapes. The lognormal distribution provided a good fit to the cell volume distribution of the foam. Therefore, it was also chosen for the volume distribution of the generating spheres. The probability density function of this distribution family is given by

$$p(r) = \frac{\exp\left(-\frac{(\log r - m)^2}{2\sigma^2}\right)}{\sqrt{2\pi}\sigma r}, \quad r \geq 0, \tag{2}$$

with parameters  $m \in \mathbb{R}$  and  $\sigma > 0$ .

To determine the model parameters, the geometric characteristics of the foam cells were compared to the characteristics of the tessellation cells using the following distance measure. Denote by  $\hat{c}_i, i = 1, \dots, 8$ , the eight quantities given in Table 1 and let  $c_i(m, \sigma), i = 1, \dots, 8$ , be estimates of these quantities obtained from Laguerre tessellations with parameters  $m$  and  $\sigma$  for the sphere volume distribution. The optimal parameters are those, for which the relative distance

$$d_{m,\sigma} = \sqrt{\sum_{i=1}^8 \left(\frac{\hat{c}_i - c_i(m, \sigma)}{\hat{c}_i}\right)^2} \tag{3}$$

is minimized. In the application, the optimal parameters for the volume distribution were found to be  $m = 1.0508$  and  $\sigma = 0.2849$ . Visualizations of one of the CT images and of the fitted model are shown in Fig. 2.

Until now, we only considered the cell system of the foam. In a second modeling step, the actual open- or closed-cell foam model is derived from the edges or facets of the tessellation model by morphological operations (Soille 1999). When modeling open-cell foams, the cross-section thickness along the strut is usually kept constant.

Locally variable strut thickness was considered by Kanaun and Tkachenko (2008) and Liebscher and Redenbach (2013). Here, the strut thickness is modeled as a polynomial of the distance  $x$  from the strut center to the adjacent nodes. In Liebscher and Redenbach (2013) it turned out that a polynomial of the form

$$p(x) = ax^8 + bx^4 + cx^2 + d, \tag{4}$$

$a, b, c, d \in \mathbb{R}$  results in the best model for the strut thickness.

### 3 Determination of Linear Elastic Properties

#### 3.1 Stiffness Tensor

In order to compute the linear elastic properties of metal foam, mesoscopic volume elements were created with the microstructure generator and boundary conditions yielding an upper (kinematic uniform boundary conditions, KUBC) and a lower bound (static uniform boundary conditions, SUBC) for the compliance tensor (Hazanov and Huet 1994) were applied. This procedure is often utilized in the context of homogenization techniques (see e.g. Kanit et al. 2003; Ostoja-Starzewski 2007), but mainly for the determination of the size of a statistically representative volume element (RVE). The size of the RVE is defined by the element size, for which these two bounds converge against the same value. Therefore, the mechanical properties of the RVE are theoretically deterministic – in the sense of being accurate enough to represent the mean constitutive response (Drugan and Willis 1996).

It is well known that these homogenization techniques are based on the condition that the scale of the microstructure and the scale of the observed mechanical properties can be separated due to a large difference in their characteristic lengths. Unfortunately, the characteristic length scale of metal foam is in many applications not much smaller than the characteristic length scale of the structure to be investigated. For these reasons, homogenization schemes can not be applied. One has to consider stochastic volume elements (SVE) instead. In this case the above mentioned method of loading different boundary conditions can still be adopted yielding so-called apparent properties (Huet 1990)

$$\begin{aligned}\sigma_0 &= \mathbf{C}_{\text{apparent}}^{\text{SUBC}} \langle \epsilon \rangle, \\ \langle \sigma \rangle &= \mathbf{C}_{\text{apparent}}^{\text{KUBC}} \epsilon_0,\end{aligned}\quad (5)$$

where  $\langle . \rangle$  denotes the volume average,  $\sigma$  and  $\epsilon$  the stress and strain tensor and  $\sigma_0$  and  $\epsilon_0$  the imposed stresses and strains according to SUBC and KUBC, respectively. When ensemble averaged, the apparent properties yield bounds for the effective material properties of interest. For a larger SVE the bounds become closer and their scatter smaller (Ostoja-Starzewski 2007). Here, the aim is not to compute effective properties, but to model the scatter in the stiffness tensor and to predict its consequences on the natural frequencies. Under assumption of the Hill condition, the following inequality holds for the apparent stiffness tensor  $\mathbf{C}_{\text{app}}$  (Hazanov and Huet 1994):

$$\mathbf{C}_{\text{apparent}}^{\text{SUBC}} \leq \mathbf{C}_{\text{app}} \leq \mathbf{C}_{\text{apparent}}^{\text{KUBC}}, \quad (6)$$

100 SVEs with a side length of 25 mm are generated and each SVE is loaded by different load cases for the boundary conditions mentioned above and solved with the help of the finite element method. After that, the apparent material parameters are calculated from the results.

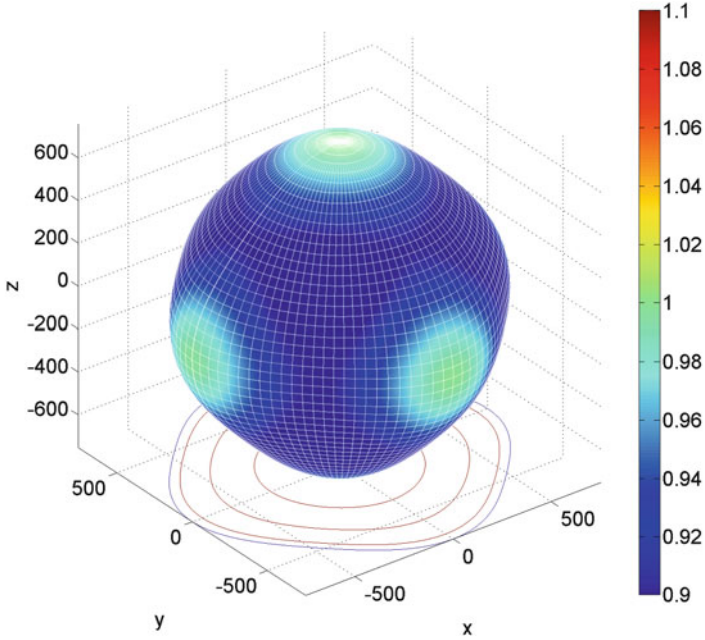


Fig. 3 Isotropic-orthotropic behavior: Young’s modulus in different spatial directions

### 3.2 Material Symmetry

Additionally, the symmetry of the elastic properties can be investigated. It turns out that the symmetry properties depend on the size of the SVE: for a small size, cubic symmetry with three independent linear elastic material parameter is obtained, while for a larger SVE size, isotropic behavior is found. This can be illustrated graphically by projecting the ensemble averaged compliance tensor on space directions  $\mathbf{d} = [x, y, z]^T$  and inverting in order to obtain a directional dependent Young’s modulus:

$$E(\mathbf{d}) = [(\mathbf{d} \otimes \mathbf{d}) : \mathbf{S} : (\mathbf{d} \otimes \mathbf{d})]^{-1}. \tag{7}$$

While a cube represents cubic symmetry, a sphere means isotropic symmetry. Figure 3 shows the relative deviation of the directional dependent Young’s modulus from the average value in the three space directions,

$$\frac{1}{3} (E([1, 0, 0]^T) + E([0, 1, 0]^T) + E([0, 0, 1]^T)). \tag{8}$$

It indicates that there is a mixture of both symmetries for the mentioned SVEs with a side length of 25 mm.

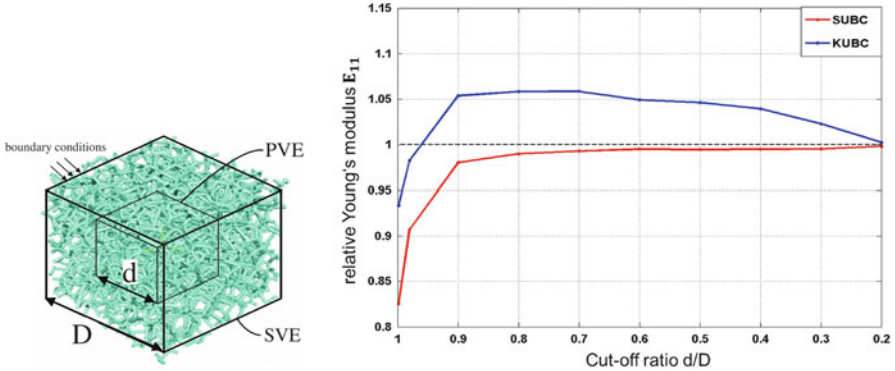


**Fig. 4** Definition of the partial volume element (PVE) and the behavior of the relative Young's modulus as a function of ratio  $d/D$

### 3.3 Partial Volume Averaging

As discussed in Sect. 3.1 we obtain a lower and upper bound of the stiffness tensor. For the determination of an apparent boundary effect free stiffness tensor, the influence of the boundary conditions has to be eliminated. In order to omit the border areas of the SVE, which are mainly influenced by the boundary conditions, strains and stresses are averaged over an inner partial volume of the SVE. The center point of the partial volume element (PVE) coincides with that of the SVE.

Defining the edge length  $D$  of the SVE and  $d$  of the PVE, the behavior of the relative Young's modulus as a function of the ratio  $d/D$  is illustrated in Fig. 4. By reducing the ratio  $r_{dD} = d/D$ , the influence of the boundary conditions is minimized and as a result the stiffness tensors for SUBC and KUBC converge against the same value.

Contrary to the expectation that the upper bound should become lower by increasing  $r_{dD}$ , both bounds first increase and then approach for  $r_{dD} < 0.9$ . The reason for this characteristic curve lies in the microstructure of the foam. The SVE is cut out from a surrounding network causing cut struts in the border area. This reduces the stiffness in that area. In the inner part of the SVE struts are not cut and the interior is stiffer than the exterior. This leads us to a paradox: On the one hand we want to determine the material parameters without influence of the boundary conditions and on the other hand we have to consider the boundary effect because of the difference of the stiffness tensor in the inner and outer part of a SVE.

The same 100 SVEs of Sect. 3.1 are used to interpolate the results from the finite element method to the predefined side surfaces of the PVE. The interpolated results are used to calculate the material parameters inside the PVE.



### 3.4 Two Section Model

Due to the difference in stiffness shown in the interior and exterior of a SVE, it is not completely correct to determine material parameters by averaging over the entire volume. This would be associated with the assumption that the stiffness is constant over the volume.

For a more accurate mapping of real foams, the apparent stiffness tensor  $\mathbf{C}_{\text{app}}$  which is assumed as the mean value of  $\mathbf{C}_{\text{apparent}}^{\text{SUBC}}$  and  $\mathbf{C}_{\text{apparent}}^{\text{KUBC}}$  is interpreted as the mean value of the stiffness tensor of the outer and inner part. For the interior the stiffness is calculated at  $r_{dD} = 0.2$  in Fig. 4. The boundary between the interior and exterior is determined by the average length of the cut struts. The stiffness in the border area is calculated with the model of springs connected in series. The Young's modulus is then described by the formula

$$\frac{1}{E_{SVE}} = \frac{p_i}{E_{\text{interior}}} + \frac{1 - p_i}{E_{\text{exterior}}}, \quad (9)$$

where  $p_i$  is the percentage of the inner edge length and  $E_{SVE}$  is Young's modulus obtained from  $\mathbf{C}_{\text{app}}$ .

### 3.5 Variable Strut Thickness

In reality, the thickness of each strut varies and can be described by a polynomial. Therefore every strut is now divided in several beams. The thickness of each beam is adapted to the polynomial in Eq. (4).

For the Duocel© copper foam eight beams for every strut are used to find a compromise between the accuracy of modeling and calculation time.

## 4 Statistical Evaluation of Material Properties

### 4.1 Determination of the Distribution Function

Relative frequencies for the boundary effect free apparent material properties are shown in Fig. 5. From the relative frequencies, empirical distribution functions can be obtained.

### 4.2 Determination of the Correlation Functions

As the linear-elastic material parameters and the mass density will serve as input parameters for structural computations, they are represented as random fields. The

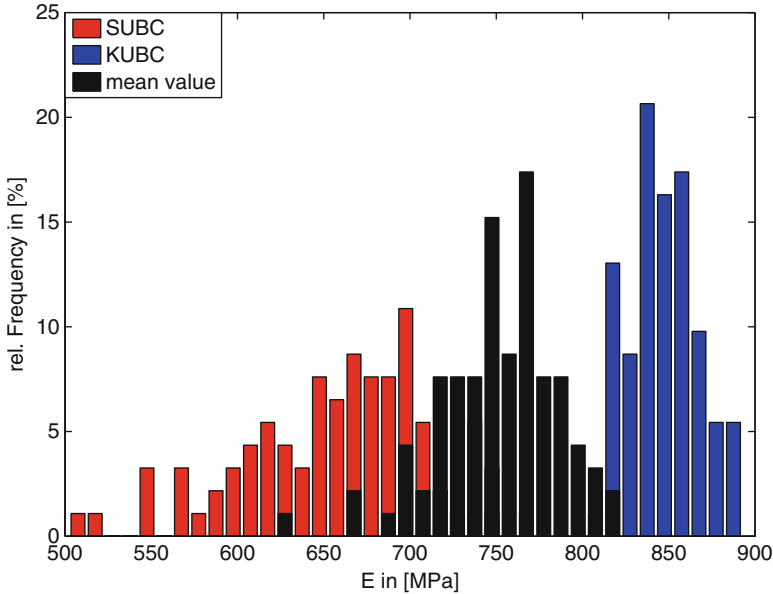


**Fig. 5** Histogram of the boundary effect free Young's modulus

random fields are assumed to be homogeneous as a consequence of the homogeneity of the generated microstructure geometry. In order to find the correlation functions for the linear-elastic material parameters, 15 beam structures ( $100 \times 10 \times 10$  mm) made of foam are analyzed by a method of moving SVEs: SVEs of the same size are cut out of each of these beams at different positions along the longitudinal axis. For each SVE the material parameters are calculated as functions of the center point coordinate  $x$  on the longitudinal axis.

For the computation of the autocorrelation function, the 15 realizations are made mean free and scaled to unit variance. After that, the autocorrelation function is obtained by taking the mean value over all 15 realizations at each distance  $\Delta$ . The results for the Young's modulus  $E$ , shear modulus  $G$ , bulk modulus  $K$  and mass density  $\rho$  are shown in Fig. 6. It can be seen from these results that the autocorrelation functions approach zero with increasing distance. Moreover, the correlation length is rather small.

Figure 6 also indicates that the autocorrelation functions reveal a similar behavior. Therefore, the autocorrelation functions have been fitted to the expression

$$C(x) = e^{-c|x|} (1 - c|x|), \quad (10)$$

which has been proposed in Liebscher et al. (2012). In Fig. 7 the fitted autocorrelation function is plotted.

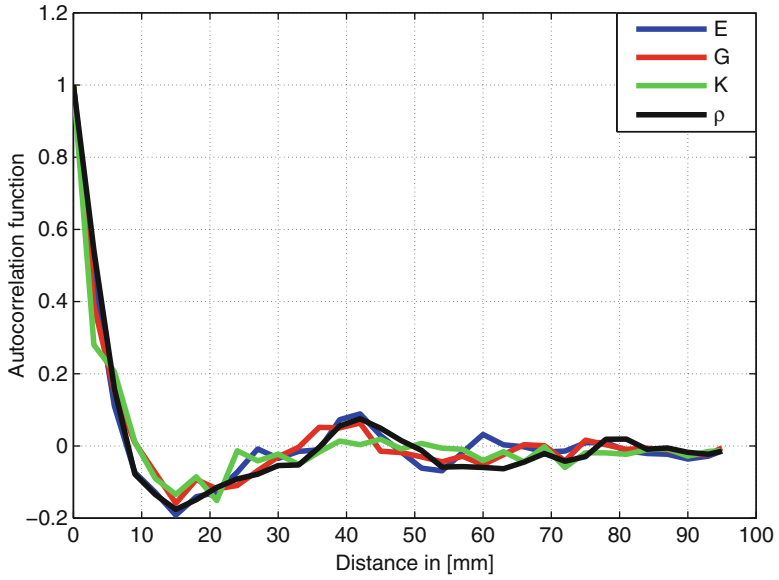


Fig. 6 Estimated autocorrelation functions

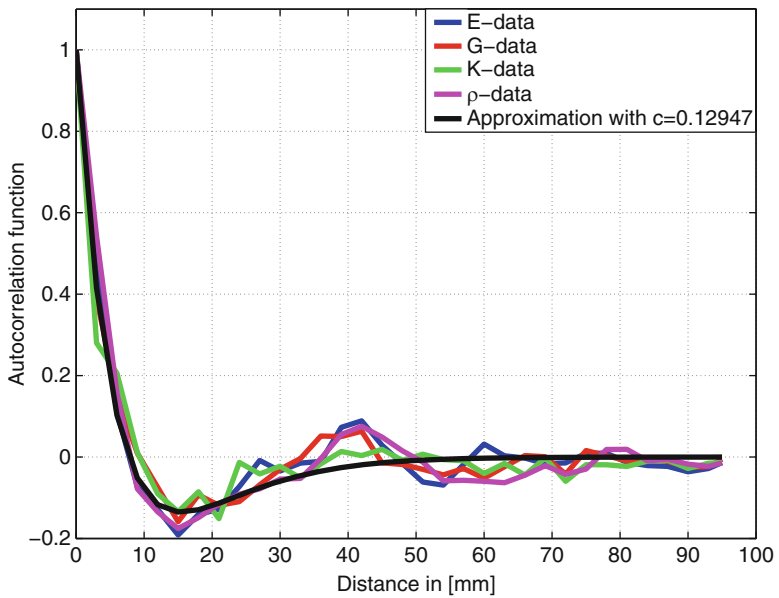


Fig. 7 Approximation of the autocorrelation functions

In the same manner, the crosscorrelation functions can be obtained. It turns out that the material parameters are almost uncorrelated.

The random fields for the material parameters and the mass density are described by the empirical distribution functions and the autocorrelation functions. They are discretized by a truncated KLE. Samples of the random variables involved in the KLE are generated iteratively by adapting the empirical marginal distribution. For this, a procedure described in Phoon et al. (2005) is applied.

## 5 Validation of the Implemented Model

### 5.1 Comparison with Finite Element Method

The bending eigenfrequencies from foam beams calculated by the finite element method (FEM) are compared with the results obtained from the method presented in this article. 100 Duocel<sup>®</sup> copper foam beams are generated with the dimensions  $255 \times 15 \times 15$  mm. Their eigenfrequencies are calculated with the help of the FEM-software ABAQUS<sup>®</sup>. The mean values and the coefficient of variation of the results are listed in Table 2.

As the next step, a SVE with side length 15 mm is cut out of each generated copper foam beam, so that from 100 SVEs the material parameters can be calculated using the presented method in Sect. 3.1. With the obtained material parameters the eigenfrequencies of beams are calculated using Timoshenko theory and Monte Carlo simulation. This procedure is named *one section model* (OSM), because stresses and strains are averaged over the whole volume of a SVE.

To investigate the effects of the *two section model* (TSM) from Sect. 3.4, the material parameters are calculated using the PVE. The percentage of the inner edge length  $p_i$  from Eq. (9) is 0.8613. In a Monte Carlo simulation the bending stiffness  $EI$  is split for the interior and exterior of the foam beam. The results of these three methods are summarized in Table 2.

OSM and FEM yield similar results for the first two bending eigenfrequencies. The deviation between these two methods becomes larger for higher bending modes.

**Table 2** Young's modulus and Eigenfrequencies using FEM, OSM and TSM

	$E_{SVE}$	$E_{interior}$	$E_{exterior}$
MPa (c.o.v.)	615 (10.2 %)	977 (7.9 %)	193 (22.9 %)
	Bending frequencies [Hz] (c.o.v.)		
	FEM	OSM	TSM
1st bending mode	173 (1.6 %)	173 (1.4 %)	175 (1.1 %)
2nd bending mode	468 (1.4 %)	465 (1.7 %)	474 (1.1 %)
3rd bending mode	897 (1.1 %)	881 (1.7 %)	900 (1.5 %)
4th bending mode	1,432 (1.4 %)	1,398 (1.7 %)	1,444 (1.5 %)

**Table 3** Material parameters for Cu Duocel®

Property	$\mu$	$\sigma$	COV (%)
Young's modulus	737 MPa	42 MPa	5.7
Shear modulus	239 MPa	13 MPa	5.3
Mass density	1,047 kg/m <sup>3</sup>	53 kg/m <sup>3</sup>	5

**Table 4** Comparison for the beam of Cu Duocel® (250 × 25 × 25 mm)

	Bending frequencies [Hz] (c.o.v.)			
	OSM	TSM	VST	Experiments
1st bending mode	334 (1.4 %)	332 (1.5 %)	320 (1.3 %)	314 (2.8 %)
2nd bending mode	861 (1.9 %)	866 (2.0 %)	827 (2.2 %)	761 (3.4 %)

Nevertheless the error remains less than 4 %. Also the coefficient of variation becomes larger for the OSM. The TSM is consistent to FEM even for higher frequencies with an error less than 2 %. It behaves stiffer than the OSM which is due to the stiff interior region. The coefficient of variation is relatively low for all three methods, because the deviations of the material parameter average out along the longitudinal axis of the beam.

Obviously the distinction between the different stiffnesses in the foam beam become more important for higher bending modes. The remaining error between FEM and TSM may attributed to the inaccuracy of the determination of the transition between the interior and exterior of the beam.

## 5.2 Comparison with Experiments

In this section, the natural frequencies of beams made of Cu Duocel® are predicted by OSM, TSM, a model using the variable strut thickness (VST) and compared with experimental values. To this end, 25 beams of size 25 × 25 × 250 mm are investigated experimentally in two ways. First, the density is determined via optical measurements and second, experimental modal analysis was performed.

The linear-elastic material properties of Cu Duocel® and the mass density were calculated with the proposed mesoscopic model. The input parameter to this model were

- The material data of copper,
- The geometric characteristics estimated from the CT data of 10 Cu Duocel® cubes of length 25 mm,
- The cross section shape of the beam network.

The result of the mesoscopic modeling is given in Table 3. Table 4 compares the first two bending frequencies obtained from Monte Carlo simulations and experiments. The mean values obtained by OSM and TSM are larger than the experimentally determined mean values. This is due to the constant strut thickness. The results

between OSM and TSM does not differ significantly because the influence of the border area from the TSM is low compared to the cross-sectional area from the beam. The VST using the polynomial from Sect. 2.2 results in a better accordance.

The remaining difference between VST and experiments could be related to experimental conditions and the simplified microstructure geometry of the model (e.g. ignoring the anisotropy).

## 6 Conclusions

In this paper, a novel model for structures made of metal foam is developed. It consists of an interior region and a boundary region. For both regions, non-Gaussian random fields are identified by averaging stresses and strains on statistical volume elements that represent the heterogeneous network of struts.

Comparisons of simulations with the novel two region model and numerical as well as experimental results demonstrate that highly accurate dynamical properties can be obtained with the proposed model. Moreover, it has been shown that the random variation of the strut thickness constitutes an important parameter that has to be taken into account in order to produce accurate predictions of macroscopic properties.

The proposed model can be refined to take the anisotropy of the network geometry into account. It can be applied to the study of other macroscopic properties of metal foams, notably their damping and crushing behavior. Finally, the proposed model can be applied to other classes of materials with heterogeneous microstructure as well.

**Acknowledgements** This work was supported in part by the German Research Foundation (DFG) under grants RE 3002/1-1 and PR 1114/10-1.

## References

- Aurenhammer F (1987) Power diagrams: properties, algorithms and applications. *SIAM J Comput* 16:78–96
- Di Paola F (2011) Modélisation multi-échelles du comportement thermo-élastique de composites à particules sphériques. Dissertation, Ecole Centrale de Paris
- Dirrenberger J, Forest S, Jeulin D (2014) Towards gigantic RVE sizes for 3D stochastic fibrous networks. *Solids Struct* 51:359–376
- Drugan WJ, Willis JR (1996) A micromechanics-based nonlocal constitutive equation and estimates of representative volume element size for elastic composites. *J Mech Phys Solids* 44(4):497–524
- Fraunhofer ITWM, Department Image Processing (Hrsg.) (2006) MAVI – modular algorithms for volume images. Department Image Processing, Fraunhofer ITWM, Kaiserslautern. <http://www.mavi-3d.de>
- Gibson LJ, Ashby MF (1997) Cellular solids – structure and properties. Cambridge University Press, Cambridge

- Guilleminot J, Noshadravan A, Soize C, Ghanem RG (2011) A probabilistic model for bounded elasticity tensor random fields with application to polycrystalline microstructures. *Comput Methods Appl Mech Eng* 200:1637–1648
- Hardenacke V, Hohe J (2009) Local probabilistic homogenization of two-dimensional model foams accounting for micro structural disorder. *Int J Solids Struct* 46:989–1006
- Hardenacke V, Hohe J (2010) Assessment of space division strategies for generation of adequate computational models for solid foams. *Int J Mech Sci* 52:1772–1782
- Hazanov S, Huet C (1994) Order relationships for boundary conditions effect in heterogeneous bodies smaller than the representative volume. *J Mech Phys Solids* 42(12):1995–2011
- Huet C (1990) Application of variational concepts to size effects in elastic heterogeneous bodies. *J Mech Phys Solids* 38(6):813–841
- Kanaun S, Tkachenko O (2007) Representative volume element and effective elastic properties of open cell foam materials with random microstructures. *J Mech Mater Struct* 2(6):1607–1628
- Kanaun S, Tkachenko O (2008) Effective conductive properties of open-cell foams. *Int J Eng Sci* 46:551–571
- Kanit T, Forest S, Galliet I, Mounoury V, Jeulin D (2003) Determination of the size of the representative volume element for random composites: statistical and numerical approach. *Int J Solids Struct* 40:3647–3679
- Lautensack C (2008) Fitting three-dimensional Laguerre tessellations to foam structures. *J Appl Stat* 35(9):985–995
- Liebscher A, Redenbach C (2013) Statistical analysis of the local strut thickness of open cell foams. *Image Anal Stereol*. Accepted for publication 32:1–12
- Liebscher A, Proppe C, Redenbach C, Schwarzer D (2012) Uncertainty quantification for metal foam structures by means of digital image based analysis. *Probab Eng Mech* 28:143–152
- Ohser J, Schladitz K (2009) 3D images of materials structures – processing and analysis. Wiley, Heidelberg
- Ostoj-Starzewski M (2007) Microstructural randomness and scaling in mechanics of materials. Chapman & Hall/CRC, Boca Raton
- Ostoj-Starzewski M (2011) Stochastic finite elements: where is the physics? *Theor Appl Mech* 38:379–396
- Phoon KK, Huang SP, Quek ST (2005) Simulation of strongly non-Gaussian processes using Karhunen-Loève expansion. *Probab Eng Mech* 20:188–198
- Redenbach C (2009) Microstructure models for cellular materials. *Comput Mater Sci* 44:1397–1407
- Soille P (1999) Morphological image analysis. Springer, Berlin
- Stoyan D, Kendall, WS, Mecke J (1995) Stochastic geometry and its applications, 2nd edn. Wiley, Chichester
- Zhu HX, Hobdell JR, Windle AH (2000) Effects of cell irregularity on the elastic properties of open-cell foams. *Acta Mater* 48(20):4893–4900